Since January 2020 Elsevier has created a COVID-19 resource centre with free information in English and Mandarin on the novel coronavirus COVID-19. The COVID-19 resource centre is hosted on Elsevier Connect, the company's public news and information website.

Vaccine 39 (2021) 7044–7051

Contents lists available at ScienceDirect

Vaccine

journal homepage: www.elsevier.com/locate/vaccine

Evaluation of a downstream process for the recovery and concentration of a Cell-Culture-Derived rVSV-Spike COVID-19 vaccine candidate

Arik Makovitzki [a,1], Elad Lerer [a,1], Yaron Kafri [a], Yaakov Adar [a], Lilach Cherry [a], Edith Lupu [a], Arik Monash [a], Rona Levy [a], Ofir Israeli [b], Eyal Dor [a], Eyal Epstein [a], Lilach Levin [a], Einat Toister [a], Idan Hefetz [a], Ophir Hazan [a], Irit Simon [a], Arnon Tal [a], Meni Girshengorn [a], Hanan Tzadok [a], Osnat Rosen [a], Ziv Oren [a,*]

[a] Department of Biotechnology, Israel Institute for Biological Research, 24 Reuven Lerer St., Nes-Ziona, Israel
[b] Department of Biochemistry and Molecular Genetics, Israel Institute for Biological, Research, 24 Reuven Lerer St., Nes-Ziona, Israel

ARTICLE INFO

Article history:
Received 3 May 2021
Received in revised form 17 October 2021
Accepted 17 October 2021
Available online 22 October 2021

Keywords:
rVSV
SARS-CoV-2
Downstream process
Endonuclease digestion
Clarification
Hollow fiber

ABSTRACT

rVSV-Spike (rVSV-S) is a recombinant viral vaccine candidate under development to control the COVID-19 pandemic and is currently in phase II clinical trials. rVSV-S induces neutralizing antibodies and protects against SARS-CoV-2 infection in animal models. Bringing rVSV-S to clinical trials required the development of a scalable downstream process for the production of rVSV-S that can meet regulatory guidelines. The objective of this study was the development of the first downstream unit operations for cell-culture-derived rVSV-S, namely, the removal of nucleic acid contamination, the clarification and concentration of viral harvested supernatant, and buffer exchange. Retaining the infectivity of the rVSV-S during the downstream process was challenged by the shear sensitivity of the enveloped rVSV-S and its membrane protruding spike protein. Through a series of screening experiments, we evaluated and established the required endonuclease treatment conditions, filter train composition, and hollow fiber-tangential flow filtration parameters to remove large particles, reduce the load of impurities, and concentrate and exchange the buffer while retaining rVSV-S infectivity. The combined effect of the first unit operations on viral recovery and the removal of critical impurities was examined during scale-up experiments. Overall, approximately 40% of viral recovery was obtained and the regulatory requirements of less than 10 ng host cell DNA per dose were met. However, while 86–97% of the host cell proteins were removed, the regulatory acceptable HCP levels were not achieved, requiring subsequent purification and polishing steps. The results we obtained during the scale-up experiments were similar to those obtained during the screening experiments, indicating the scalability of the process. The findings of this study set the foundation for the development of a complete downstream manufacturing process, requiring subsequent purification and polishing unit operations for clinical preparations of rVSV-S.

1. Introduction

The current COVID-19 pandemic caused by severe acute respiratory syndrome coronavirus 2 (SARS-CoV-2) presented a significant challenge for the rapid development and scaled-up mass production of an efficient vaccine as the means to control the pandemic. Several different vaccination strategies have been developed in the last year against SARS-CoV-2, including nucleic acid (DNA and RNA), virus-like particle, recombinant protein, peptide, inactivated virus, and viral vector (replicating and non-replicating) approaches [1]. Viral vector technology involves the delivery of one or more genes that encode a target antigen within an unrelated, engineered virus. The viral vector can be replication-competent (live attenuated) or replication-deficient [2].

Vesicular stomatitis virus (VSV) is a member of the Rhabdoviridae family that primarily affects rodents, cattle, swine, and horses. Despite its broad host range, naturally occurring human infections with VSV are rare [3]. VSV has a rigid "bullet" shape. The virion has

Abbreviations: ACE2, angiotensin-converting enzyme 2; DO, dissolved oxygen; DSP, downstream process; hc-DNA, host cell DNA; HCP, host cell protein; HF-TFF, hollow fiber-tangential flow filtration; HR, horseradish peroxidase; MEM, minimal essential medium; MOI, multiplicities of infection; MT, multi-tray; MWCO, molecular weight cutoff; NTU, nephelometric turbidity units; PES, polyethersulfone; PFU, plaque-forming units; rVSV-S, recombinant vesicular stomatitis virus-ΔG-spike; SFM, serum-free medium; TMP, transmembrane pressure.

* Corresponding author.
E-mail address: zivo@iibr.gov.il (Z. Oren).

[1] These authors have contributed equally to this work.

https://doi.org/10.1016/j.vaccine.2021.10.045
0264-410X/

a lipid envelope decorated with glycoprotein (G) spikes that enclose a nucleocapsid composed of RNA plus nucleoprotein (N) and an associated matrix formed by (M) proteins [4]. Intact virions are approximately 70 nm in diameter and 180 nm long [5]. Recombinant vesicular stomatitis virus (rVSV) is a highly suitable vector-vaccine platform. rVSV elicits strong humoral and cellular immune responses towards expressed heterologous antigens, rapidly confers long-term immunity [6], has a low probability of pre-existing immunity in vaccine recipients [2], and is sensitive to IFN-α/β, thus contributing to its safety [7]. The rVSV platform was established as a safe and efficacious live-attenuated vaccine and vector for the prevention or treatment of infectious diseases and cancer [8].

rVSV-ΔG-spike (rVSV-S) is a recombinant replication-competent VSV-based vaccine candidate under development by the Israel Institute for Biological Research (IIBR) that is currently in phase II of clinical trials (1×10^5 –1×10^8 plaque-forming units (PFU)/dose, prime-boost, https://clinicaltrials.gov/ct2/show/NCT04608305). rVSV-S expresses the SARS-CoV-2 spike protein instead of the glycoprotein (G) of VSV [9]. The SARS-CoV-2 spike protein binds to the host cell receptor angiotensin-converting enzyme 2 (ACE2), mediating viral cell entry [10]. The total length of spike protein is 1273 amino acids, and its molecular weight is 180–200 kDa. Spike protein trimers visually form a characteristic bulbous, crown-like halo surrounding the viral particle [11]. rVSV-S resembles the SARS-CoV-2 in spike expression properties, antigenicity, and ability to induce neutralizing Th1-favored antibodies. Moreover, a single-dose vaccination of a golden Syrian hamster model with rVSV-S elicited a safe, effective, and sufficient neutralizing antibody response against SARS-CoV-2 challenge. The vaccination protected SARS-CoV-2 inoculation, as manifested by reduced morbidity, lung protection, and rapid viral clearance [9]. Additionally, recent work demonstrated the induction of efficacious and protective immunity in mice using a VSV-eGFP-SARS-CoV-2 vector [12].

Bringing rVSV-S to clinical trials requires the development of a downstream process (DSP) suitable for scale-up to eliminate impurities, either process-related (e.g., DNase, extractables, and leachables) or product-related (e.g., host cell proteins (HCPs) and host cell DNA (hc-DNA)). The ultimate goal of a DSP is to obtain sufficient product with high purity, potency, and quality that can meet the stringent guidelines of the regulatory authorities.

The DSP of cell-culture-derived viral vaccines involves several unit operations. The first unit operations include, in most cases, endonuclease digestion of the harvested supernatant, the clarification of large particles, concentration and buffer exchanges, and initial purification. Advanced unit operations include purification, polishing, and sterile filtration [13]. To our knowledge, no previously published study has described the systematic development of a DSP for rVSV. However, Ausubel et al. and two patents describe a DSP for rVSV. The DSP described by Ausubel et al. [14] is composed of a filter train clarification step, endonuclease digestion, anion-exchange chromatography, TFF, and sterile filtration. The first DSP patent is composed of two stages of clarifications (centrifugation and filtration), anion-exchange membrane adsorber chromatography, hollow fiber-tangential flow filtration (HF-TFF), and sterile filtration [15]. The second DSP patent is composed of filter clarification, endonuclease digestion, HF-TFF, and sterile filtration [16]. The three rVSV DSPs differ over the DNA removal stage and anion-exchange chromatography and share the clarification, TFF, and sterile filtration processing stages. During TFF, the cross-flow at the membrane surface creates a tangential sweeping action that reduces gel layer formation and membrane fouling [17]. Viral particles are enriched on the retentate side of the membrane, while water and small molecular weight molecules are removed with the permeate. This offers the possibility of washing off impurities, thus achieving greater levels of purity [18]. HF membranes are the preferred modules for TFF concentration as well as for buffer exchange (diafiltration) of viruses because HF membranes provide wider flow paths resulting in lower turbulence and shearing stress inside the feed channels [19,20].

The objective of this study was the development of the first downstream unit operations for a cell-culture-derived rVSV-S vaccine candidate, namely, endonuclease digestion, depth and membrane filter clarification, and concentration and buffer exchange. The suitable conditions to minimize shear-stress-induced lysis of the enveloped rVSV-S and denaturation or shedding of the large, membrane protruding spike protein during HF-TFF were thoroughly examined. A series of screening experiments examined the sensitivity of rVSV-S to shear stress and established suitable operating conditions for the scale-up of the first unit operations. Scale-up experiments demonstrated the combined effect of the first unit operations on rVSV-S infectivity recovery and load reduction of critical impurities such as HCPs and hc-DNA. We further evaluated the possibility to improve rVSV-S recovery and the removal of impurities using a flush of the system after HF-TFF and the addition of a second stage of HF-TFF. The findings of this study set a framework for subsequent purification steps (i.e. chromatography) for clinical preparations of rVSV-S, as described in our article [21].

2. Materials and methods

2.1. Cell culture and virus production

Production of rVSV-S in a multi-tray (MT) - rVSV-S virus was replicated in Vero cells (WHO Vero RCB 10–87) using serum-free medium (SFM) (FLEX20, Biological Industries, Israel). Vero cells were seeded into 6342 cm^2 MTs (NUNC EasyFill Cell Factory System, Thermo Fisher Scientific, cat. # 140400) at an initial density of 5000 cells/cm^2 and a total volume of 1000 ml SFM FLEX20 medium. Typically, 3 to 6 MTs were grown in parallel, resulting in a working volume of 3 to 6 L. Cells were grown to confluence in the MT at 37 °C, 5% CO_2, then infected with an estimated 0.1 multiplicities of infection (MOI) of rVSV-S. The rVSV-S replication reached a plateau at 72 h in the MT at 37 °C, 5% CO_2, and culture medium supernatant was harvested into 3–6 one-liter flasks.

Production of rVSV-S in a bioreactor - For each bioreactor, 3–6 MTs containing 3–6 $\times$ 10^9 Vero cells were washed with PBS, trypsinized using recombinant trypsin (10 mg/ml, Biological Industries, Bet-Haemek), and seeded into a bioreactor containing Fibra-Cel disks (Eppendorf) with SFM FLEX20. Following the attachment of the cells to the Fibra-Cel disks, the cells continued to expand under the following conditions: 37 °C, pH 7.1, and gentle agitation. Six days after the Vero cells were seeded in the bioreactor, they were infected by rVSV-S (MOI $\sim$ 0.1). The rVSV-S replication reached a plateau at 48 h in the bioreactors following which the culture medium supernatant from the infected cells was harvested into a 5-liter bag (Flexboy, Sartorius Stedim Biotech, GmbH).

2.2. Endonuclease digestion of host cell DNA (hc-DNA)

MT and bioreactor harvested supernatants were subjected to endonuclease digestion using Denerase endonuclease (20804–5 M, GMP Grade, c-LEcta, Germany). Digestion was performed at 40 U/ml, 60 U/ml, or 80 U/ml in the presence of 2 mM $MgCl_2$ (MA110, Spectrum) for 1, 2, or 3 h at 37 °C under constant and mild agitation. At the end of digestion time endonuclease activity was inhibited with 10-fold excess EDTA.

2.3. Clarification of viral harvested supernatant

Prior to TFF experiments, the endonuclease-digested viral harvested supernatant was clarified by a filter train of decreasing pore sizes. For the clarification of cells and cell debris harvested from the MT supernatant, filters with pore sizes of 3 μm (Sartopure PP3, size 4, 0.018 m^2, polypropylene, Sartorius) 1.2 μm (Sartopure PP3, size 4, 0.013 m^2, polypropylene, Sartorius) and 0.2 μm (Sartopore platinum, size 4, 0.021 m^2, polyethersulfone (PES), Sartorius) were applied at a flow rate of 150 ml/min. For the clarification of the supernatant from the bioreactors, filters with pore sizes of 3 μm (Sartopure PP3, size 5, 0.036 m^2, polypropylene, Sartorius) 1.2 μm (Sartopure PP3, size 5, 0.026 m^2, polypropylene, Sartorius) and 0.2 μm (Sartopore platinum, size 7, 0.065 m^2, PES, Sartorius) were applied at a flow rate of 250 ml/min. Filters were previously flushed and conditioned with working buffer containing 4% D-trehalose (Pfanstiehl, Zug, Switzerland) and 100 mM NaCl (Merck) in 20 mM Tris-HCl (Merck), pH 7.2.

The turbidity of the clarification samples was measured using a turbidity meter (Eutech TN-100, Thermo Scientific) and is given in nephelometric turbidity units (NTU). The measurement was performed according to the manufacturer's instructions.

2.4. Tangential flow filtration on hollow fibers (HF-TFF)

The HF-TFF concentration and diafiltration stage was performed using 500 kDa, 750 kDa, and 0.1 μm molecular weight cutoff (MWCO), 225 cm^2, and 750 kDa, 850 cm^2 PES HF membrane cartridges (Cytiva, Marlborough, MA). HF-TFF was performed on a commercial ultrafiltration system (KRONOS, Solaris Biotechnology). Before the experiments, HF membranes were equilibrated with working buffer (100 mM NaCl in 20 mM Tris-HCl, pH 7.2, and one of the following sugars: 2% or 4% sucrose (Sigma-Aldrich)) and 2% or 4% D-trehalose. All filtration experiments were performed at 9 ± 2 °C and in duplicate unless otherwise specified. The cross-flow rate through the HF was expressed as shear rate in units of s^{-1}, which made it possible to scale-up or down between cartridges. The shear rate within the fiber is given by Equation: $\gamma = 4q/\pi R^3$ where γ is shear rate (s^{-1}), Q is the volumetric flow rate through the fiber lumen (cm^3/s per fiber), and R is fiber radius (cm). The endonuclease-digested and clarified cell culture harvested supernatant was concentrated 3–4-fold by volume (to 300 ml) and then diafiltered against 5 × 300 ml of working buffer. After achieving the desired diafiltration volume, the TFF loop was completely drained and the virus in the retentate was recovered. Samples of the final retentate and permeate were taken to assess the process recovery as well as the clearance of processing impurities. Between experiments, HF cartridges were cleaned by flushing with water (10 min, 10,000 s^{-1}), NaOH (0.5 M, Merck, 30 min, 10,000 s^{-1}), water (5 min × 2, 10,000 s^{-1}), and Tris-HCl (1 M, pH 7.2, Merck, 10 min, 10,000 s^{-1}). Cartridges were stored in a solution of sodium hydroxide (0.1 M).

2.5. Infectivity assay

The infectivity assay was performed as previously described [9]. Vero E6 cells were seeded in 6-well plates (7×10^5 cells/well) and grown overnight in a growth medium. Serial dilutions of rVSV-S were prepared in minimal essential medium (MEM) and used to infect Vero E6 monolayers in duplicate (200 μl/well). Plates were incubated for 1 h at 37 °C, 5% CO_2, to allow the virus to penetrate the cells. Then, 2 ml/well of overlay [MEM × 2 containing 0.4% tragacanth (Merck, Israel)] was added to each well and the plates were incubated at 37 °C, 5% CO_2, for 72 h. The media were then aspirated, and the cells were fixed and stained with 1 ml/well of 0.1% crystal violet solution (Biological Industries, Israel). The number of plaques in each well was determined, and the rVSV-S titer was calculated. Each assay included a positive control plate containing 6 replicates (wells) of a single, known sample dilution and 2 negative control wells with MEM that did not contain a virus. The titer in plaque-forming units (PFU)/ml for each of the samples is the average of the values calculated from the tested dilutions. The mean standard deviation of the assay was 0.05 Log_{10} PFU/ml (range of 0.02–0.11) and the mean coefficient of variation (CV) was 11% (range of 4%–18%).

2.6. Host cell protein (HCP) ELISA

The level of residual proteins of the Vero cells was measured using a Vero host cell protein (HCP) ELISA kit (Cygnus Technologies, Southport, NC, USA), following the manufacturer's instructions. A total amount of 50 μl of diluted samples were added to microtiter strips coated with an affinity-purified capture goat polyclonal anti-Vero cell antibody. The horseradish peroxidase (HRP) enzyme-labeled anti-Vero cell antibody (goat polyclonal, 100 μl) was added to wells and incubated for 2 h at 25 °C with shaking at 500 rpm. The wells were washed 4 times with wash buffer to remove any unbound reactants. An amount of 100 μl of 3,3′,5,5′ tetramethylbenzidine (TMB) solution was immediately added to the plate and incubated at 25 °C for 30 min. The reaction was stopped using 100 μl of 0.5 M H_2SO_4 stop solution and the absorbance was read at 450 nm using a CLARIOstar multi-mode reader (BMG LABTECH, Ortenberg, Germany). All standards, controls, and samples were assayed in duplicate; 2 different dilutions of the sample were tested. The residual Vero HCP concentration (ng/ml) in a tested sample was calculated by interpolation from a 4-parameter nonlinear fit regression of the standard curve after subtracting the blank.

2.7. DNA fragment size determination

DNA was extracted from the samples using a DNA QIAamp DNA Blood Mini Kit (Qiagen) according to the blood and body fluids protocol in the QIAcube robot and was recovered in a 100 μl elution volume in ddH_2O. The DNA fragment sizes were assessed using the TapeStation 4200 device (Agilent Technologies, Santa Clara, CA) with a high-sensitivity DNA screen tape.

2.8. Quantitation of Vero cell residual DNA by qPCR

The concentration of Vero cell residual DNA was determined by quantitative PCR (qPCR) using resDNASEQ™ Quantitative Vero DNA Kit, based on a TaqMan real-time qPCR technology (Applied Biosystems, Thermo Fisher Scientific). Host cell DNA was first isolated and recovered with magnetic beads using a PrepSEQ Residual DNA Sample Preparation Kit (Applied Biosystems, Thermo Fisher Scientific). A DNA standard curve was prepared by serial 10 × dilutions of the control Vero DNA. Nuclease-free water was used as a negative control. All samples were diluted in DDB (DNA Dilution Buffer). A reaction mix was prepared according to the kit's instructions and added to wells in a white 96-well plate (20 μl/well, in duplicates). Then, DNA samples (standards or unknowns) were added (10 μl/well), and the plate was transferred to a LightCycler® 96 Instrument (Roche Life Science). At the end of the reaction, the DNA concentration in the tested sample was back-calculated by interpolation from a linear regression fit of the standard curve. The assay was linear in the concentration range of 0.03–300 ng/ml. The limit of detection (LOD) and quantitation (LOQ) reached 1 ng/ml and 3.1 ng/ml, respectively. The assay had a relative standard deviation (RSD) of 4.8%.

3. Results and discussion

Endonuclease digestion, clarification, concentration, and buffer exchange are the first unit operations in most DSPs of viral vaccines [13]. Their main purposes are to reduce nucleic acid contamination and solution viscosity, to clarify large particles (microcarriers, cell debris, organelles, etc.), and to concentrate and partially remove impurities (e.g., harvested supernatant, HCPs, and hc-DNA) for subsequent purification stages. rVSV-S is a complex bioparticle covered with a lipid envelope and the bulky SARS-CoV-2 spike proteins. A series of experiments were required to apply the first unit operations for the rVSV-S DSP, with the least effect on the structural integrity and infectivity.

3.1. Endonuclease digestion of hc-DNA

Host-cell-derived DNA (hc-DNA) is part of a semi-stable chromatin hetero-complex consisting of nucleosomal arrays (DNA + histone proteins), single nucleosomes, DNA, and non-histone proteins [22]. Chromatin contamination is known to associate with the viral particles, resulting in co-purification, virus aggregation, and increased solution viscosity [23,24]. In addition, to eliminate potential oncogenes or other functional DNA sequences, the regulatory requirements set the acceptable DNA levels between 10 ng and 10 pg per dose with a size of less than 200 base pairs, depending on the type of product, medical indication, production host, and administration route [13]. Although rVSV-S do not require cell lysis, because the virus is secreted by the producer cell through a budding process [19], some hc-DNA is released into the medium by fragmented Vero cells.

The effect of nonspecific endonuclease (Denerase) concentrations and incubation time on DNA fragment size degradation, which facilitates DNA removal during TFF, was investigated. Fig. 1 depicts the determination of the size distribution of the DNA fragments following digestion at 40 U/ml, 60 U/ml, or 80 U/ml for 1, 2, or 3 h at 37 °C. Higher enzyme concentration than 40 U/ml and longer incubation than 2 h did not improve substantially DNA degradation efficiency. Due to upstream process variation, treatment with 60 U/ml endonuclease for 3 h at 37 °C was selected to ensure optimal DNA degradation.

Thus, rVSV-S harvested supernatants from 4 independent MT batches with a concentration of $2 \pm 0.5 \times 10^7$ PFU/ml were treated with endonuclease at 60 U/ml for 3 h at 37 °C. At the end of digestion time endonuclease activity was inhibited with 10-fold excess EDTA. Samples of the harvested supernatant contained 18500 ± 450 ng/ml DNA. After the endonuclease digestion, the samples contained 20 ± 13 ng/ml DNA, a reduction in the DNA concentration of 99.9%.

The infectivity assay performed after the endonuclease digestion (60 U/ml, 3 h, 37 °C) revealed that the infectivity of rVSV-S remained unchanged. Together, these results indicate that endonuclease digestion can significantly reduce the hc-DNA concentration and fragment size without impairing the infectivity of rVSV-S.

3.2. Clarification of viral harvested supernatant

Host cell debris, large aggregates, and insoluble impurities found in the harvested supernatant burden subsequent DSP unit operations. Consequently, an early clarification filter train of decreasing pore sizes is required after viral harvesting [25]. In choosing the filter train, we considered the facts that enveloped viruses, because of their lipidic envelope, are more prone to adsorption and that the maximum cell debris size, estimated using inverted microscopy, was approximately 5 μm. Thus, we chose a scalable filter train composed of 3 μm and 1.2 μm inert polypropylene depth filters, and a 0.2 μm membrane filter. Endonuclease-digested rVSV-S harvested supernatants from 6 independent MT harvested batches with a concentration of $5 \pm 3 \times 10^6$ PFU/ml were used for the clarification experiments. The results were assessed by infectivity assay and turbidity reduction. Using this filter train, a high recovery of 82 ± 5%, was obtained, similar to the obtained recovery during the clarification of lentivirus and adeno-associated virus [26], and Orf virus [27]. Turbidity values of the harvested supernatant were 14.9 ± 3 NTU and following clarification values of 6.9 ± 1.2 NTU were obtained, demonstrating approximately 50% decrease in turbidity with the different viral harvested batches.

In order to examine the efficiency of endonuclease digestion after clarification, 60 U/ml of endonuclease was added to 2 independent MT batches of rVSV-S clarified supernatant with a concentration of $2 \pm 0.5 \times 10^7$ PFU/ml. The recovery obtained using the 3 μm, 1.2 μm, and 0.2 μm filter train was 89 ± 3%, as compared to 82 ± 5% recovery obtained when endonuclease digestion was performed before clarification. At the end of digestion time (3 h at 37 °C) endonuclease activity was inhibited with 10-fold excess EDTA. Samples treated with endonuclease after clarification presented DNA removal efficiencies of 99.97%, similar to DNA removal efficiencies prior to clarification (99.9%). Considering the importance of DNA digestion to harvested supernatant viscosity reduction, in particular when upscaling the clarification process

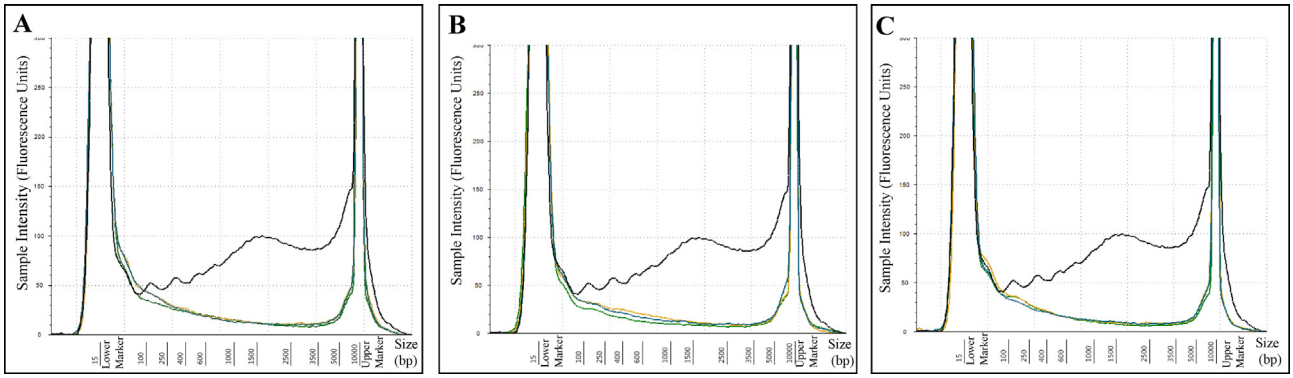

Fig. 1. Size of DNA fragments after endonuclease digestion. rVSV-S harvested supernatant was treated with nonspecific endonuclease (Denerase) at 40 U/ml (A), 60 U/ml (B) or 80 U/ml (C) in the presence of 2 mM $MgCl_2$ for 1 (blue), 2 (yellow) or 3 (green) hours at 37 °C. Control-non-digested DNA fragments (Black). Endonuclease activity was inhibited with 10-fold excess EDTA. The samples were analyzed using a TapeStation 4200 device with a high-sensitivity DNA screen tape. The high-sensitivity D5000 markers are double-stranded DNA fragments with known sizes of 15 and 10,380 bp (lower and upper marker, respectively), which are embedded in the buffer of each sample. Data are representative of two independent experiments.

[23,24,28], endonuclease treatment was performed prior to clarification in all further experiments.

3.3. HF-TFF screening

Concentration and buffer exchange (diafiltration) is an important stage in the DSP of rVSV-S to reduce viral harvested volume, achieve buffer exchanges, and reduce the impurity load for the subsequent purification stages. HF-TFF MWCO and operational parameters should be carefully selected to minimize viral particle loss and damage due to shear-stress-induced lysis of the enveloped rVSV-S and the denaturation of the protruding spike protein. In a series of screening experiments, we examined the effects of HF MWCO, shear rate, and transmembrane pressure (TMP) on membrane fouling (correlated to flux variations) and rVSV-S infectivity. Endonuclease-digested and clarified rVSV-S harvested supernatants from MTs with a concentration of $5 \pm 3 \times 10^6$ PFU/ml were used during the screening experiments.

3.3.1. Rejection of rVSV-S as a function of HF membrane MWCO

Intact rVSV is approximately 70 nm in diameter and 180 nm long [5]. To select the HF membrane with the largest pore size that rejects rVSV-S, HF with 500 kDa, 750 kDa, and 0.1 μm MWCO were selected, according to the HF manufacturer's guide. These HF membranes were screened in a preliminary study for the rejection of viral particles. Batches of 800 ml of endonuclease-digested and clarified harvested virus were concentrated 3-fold with the 500 kDa, 750 kDa, and 0.1 μm HF. For each HF, three shear rates were examined, 8000 s^{-1}, 10,000 s^{-1}, and 12,000 s^{-1}, to assess whether high shear rates could be used with complete rejection of the rVSV-S. HF rejection was examined by performing a viral infectivity assay on the permeate reservoir samples. For all shear rates examined, the 500 kDa and 750 kDa HF completely rejected the viral particles. Full permeation was observed for rVSV-S with the 0.1 μm HF, probably due to its narrow dimension of approximately 70 nm. Next, we compared Vero HCP removal by 500 and 750 kDa HF. Endonuclease-digested and clarified harvested virus (800 ml) was concentrated 3-fold and diafiltered by a factor of 5 at shear rates of 10,000 s^{-1} and 12,000 s^{-1}. HCP was reduced by 67% and 63% for 500 kDa HF at shear rates of 10,000 s^{-1}, 12,000 s^{-1}, respectively, and 75% and 82% for 750 kDa HF at shear rates of 10,000 s^{-1}, 12,000 s^{-1}, respectively. Based on these results, the 750 kDa HF, which allows the removal of larger amounts of HCP, reduces the membrane area requirements, and reduces the processing time, was chosen for further evaluation.

3.3.2. Characterization of the shear stress sensitivity of rVSV-S

To study the sensitivity of rVSV-S towards shear stress, clarified and endonuclease-digested harvested virus (300 ml) was continuously circulated on 750 kDa HF at different wall shear rates (12,000 s^{-1}, 9,000 s^{-1}, and 6,000 s^{-1}, 30 min at each shear rate) and zero flux. A continuous decline in rVSV-S infectivity was observed following the exposure to the 3 shear rates, reaching a 93 ± 5% loss of infectivity at the end of the circulation. We then evaluated the stabilizing effect of sugar additives on rVSV-S [29,30] against shear stress by repeating the study (in duplicate) after the addition of D-trehalose or sucrose at 2% or 4% (w/v). The addition of either 2% D-trehalose or 2% sucrose decreased the infectivity loss at the end of circulation to 87 ± 5%. A larger stabilizing effect was obtained with either sugar additive at 4%, decreasing the infectivity loss following circulation to 80 ± 4%. 4% D-trehalose was chosen for further studies due to its wide use as a viral vaccine stabilizer [31].

3.3.3. TMP and shear rate optimization

To select the optimal conditions during concentration and diafiltration of the clarified and endonuclease-digested rVSV-S harvested supernatant using the 750 kDa HF, a screen of rVSV-S recovery as a function of TMP and shear rate was performed. The concentration factor was 3–4 and the diafiltration factor was 5 for all conditions examined. At shear rates of 4000 s^{-1} and 6000 s^{-1} and a TMP of 0.5, a 10–15-fold reduction in the flux (expressed as $L/m^2/h$, LMH) was observed during the concentration due to fouling of the membrane. Flux reduction continued through the diafiltration, leading to the complete fouling of the membrane and the early termination of the run (data not shown). The most probable cause for the observed impediment of fluid flux is a buildup of a gel-like layer of solution components (e.g. cell debris and HCPs) on the membrane surface [32]. We, therefore, examined higher shear rates of 8000–12,000 s^{-1} while maintaining a low TMP of 0.5–1. Under these conditions, a more efficient tangential sweeping action helps to wash solution components back into the retentate, reducing the accumulation of the gel-like layer.

The results of the rVSV-S recovery for the various shear rates and TMPs examined are summarized in Table 1. No significant differences were observed between the virus recoveries and the flux versus the filtrate volume graphs at the different shear rates/TMPs examined. For all shear rates and TMPs, similar 3-fold decay in the flux during the 3–4-fold concentration was observed (data not shown), due to the formation of the gel-like layer of impurities and viral particles. During diafiltration, a fresh addition of working buffer combined with the tangential sweeping action of the cross-flow at the membrane surface prevented further fouling of the membrane and stabilized the flux. The overall processing time during the concentration and diafiltration of rVSV-S in the range of 8,000 s^{-1}-12,000 s^{-1} and a TMP of 0.5–1 was also similar.

Our results indicate the existence of a critical shear rate (8,000 s^{-1}), below which fast and complete fouling of the HF membrane occurs. Above this shear rate, there is lower fouling by solution impurities during concentration, improved tangential sweeping action during diafiltration, and optimum recovery of infectious particles. The maximal shear rate that can be used in the next scale-up step is derived from the operating capability of the TFF system, the turbulent flow conditions in the reservoir tank, and the shear sensitivity of rVSV-S.

3.4. Scaling up the rVSV-S DSP

The ability to scale-up a process is a key factor in DSP development. Thus, we scaled up our process based on the results of our screening experiments. rVSV-S was harvested from 3.5 L bioreactors instead of 1 L MTs. The average rVSV-S concentration in the bioreactors was $6 \pm 4 \times 10^8$ PFU/ml, two orders of magnitude higher than in the MTs. A filter train composed of 3, 1.2, and 0.2 μm pore sizes with a 2–3-fold larger membrane area was used for clarification. An approximately 4-fold increase (from 225 cm^2

Table 1
The effect of TMP and shear rates on rVSV-S infectivity recovery during concentration and diafiltration using a 225 cm^2 750 kD MWCO HF membrane.

TMP (Bar)	Number of experiments	Shear rate (s^{-1})	Infectivity recovery[a] (%)
0.5	3	8,000	23 ± 7
0.5	3	9,000	37 ± 16
1	3	9,000	33 ± 15
0.5	4	10,000	39 ± 15
1	3	10,000	23 ± 5
0.5	4	12,000	44 ± 20

[a] Infectivity recovery values are means ± standard error of the means.

to 850 cm^2) in the surface area of the HF membrane was used while maintaining the same membrane material, pore size, channel height, and shear rate.

Pooled harvested supernatant from 2 bioreactors was endonuclease-digested and clarified as described in the materials and methods section. The solution was divided into six 1.5 L individual runs. In each run, the solution was concentrated 4-fold and diafiltered 5 times against the working buffer (4% D-trehalose and 100 mM NaCl in 20 mM Tris-HCl, pH 7.2). The shear rate during concentration and diafiltration was set to the maximal 10,000 s^{-1} the system can reach with the scaled-up HF membrane. At these conditions, a TMP of a maximum of 0.9 bar was maintained throughout the process and the turbulence in the reservoir tank was moderate. To evaluate the contribution of the accumulated layer of rVSV-S on the HF membrane surface to the total recovery of the virus, a small volume of working buffer was used to flush the membrane surface, tubing, and reservoir after the recovery of the retentate. In addition, to investigate the effect of the second stage of concentration and diafiltration on the removal of the major product-related impurities (HCPs and hc-DNA), a pool of retentates and flushes from the 6 TFF runs of the 2 bioreactors (4 L total) was concentrated 5-fold and diafiltered 5 times against the working buffer. A scheme of the scale-up experiments is presented in Fig. 2. The recovery of infectious rVSV-S and the concentration of HCPs and hc-DNA from the first and second stages of concentration and diafiltration were determined.

Table 2 presents the viral titer and the residual levels of HCPs and hc-DNA in the three stages used in this study: endonuclease-digestion and the clarification of Vero cell harvested supernatant, first TFF stage (TFF I, 6 individual runs), and second TFF stage (TFF II, pool of the 6 retentates and flushes). The results of two independent scale-up experiments (scale-up experiments 1 and 2) are presented.

Similar recoveries were obtained in the two experiments for the three stages, despite a 4-fold higher titer in scale-up experiment 2 than in scale-up experiment 1, due to upstream process variation. Overall, approximately 60% of the viral infectivity was lost during the DSP: 20% during the endonuclease-digestion and clarification, 30% during the first TFF, and an additional 10% during the second TFF. The flushing of the membrane surface, tubing, and reservoir after the first TFF contributed only 8–15% of the recovery in each run (data not shown). This low recovery during the flushes indicates that only a small layer of rVSV-S is accumulated on the HF membrane and the efficient tangential sweeping action at a shear rate of 10,000 s^{-1}. Thus, these results may indicate the sensitivity of rVSV-S to shear stress as the reason for the 40% loss of infectivity of rVSV-S during the first and second TFF stages.

Residual HCPs and hc-DNA are the results of Vero cell breakdown following infection. The results showed that 20–30% of the

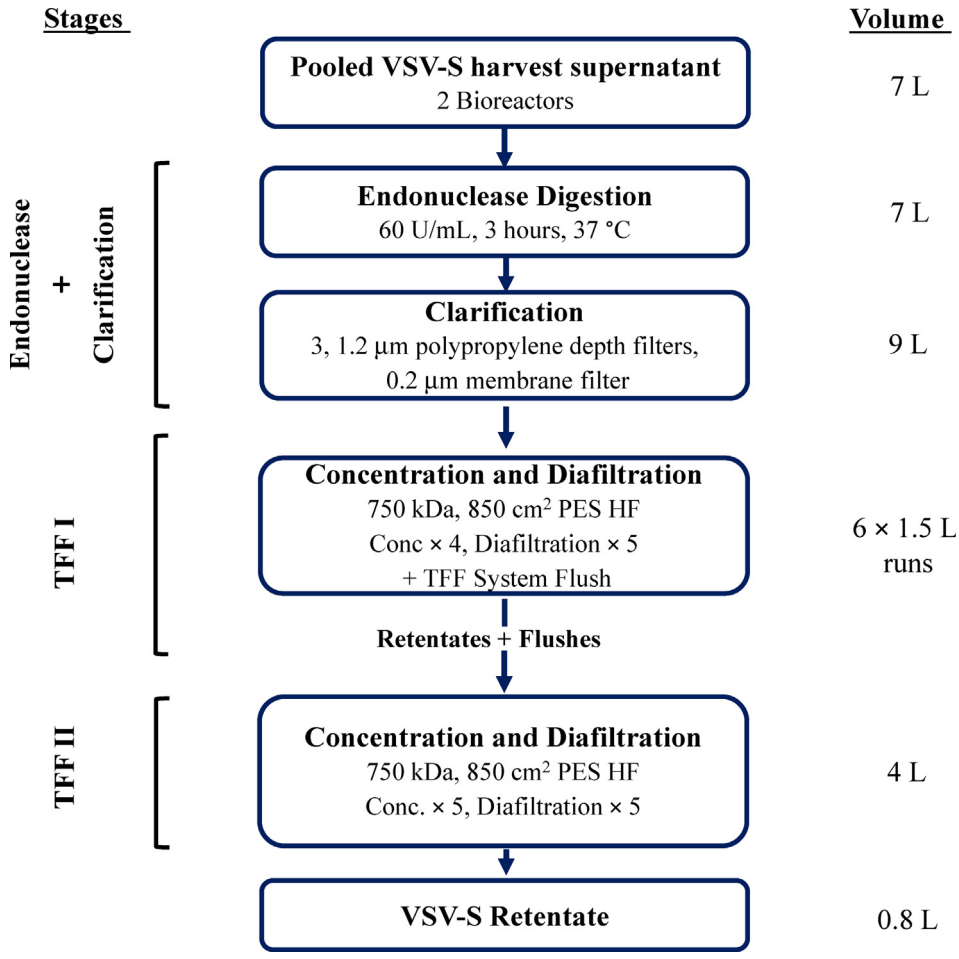

Fig. 2. Scheme of VSV-S DSP scale up experiments. Pooled VSV-S harvest supernatant from 2 bioreactors was processed through three stages: **Endonuclease and clarification**-VSV-S harvest was digested using 60 U/mL endonuclease for 3 h at 37 °C and clarified using 3, 1.2 µm polypropylene depth filters and 0.2 µm membrane filter. **TFF I**- Digested and clarified solution was divided into 6 individual runs. In each run the solution was concentrated 4-fold and diafiltrated 5 times against working buffer (4% Trehalose and 100 mM NaCl in 20 mM Tris-HCl, pH 7.2). After recovery of the retentate, working buffer was used to flush the membrane surface, tubing and reservoir. **TFF II**- A pool of retentates and flushes from the 6 TFF I runs was concentrated 5-fold and diafiltrated 5 times against working buffer.

Table 2
Performance overview of the two scaled-up rVSV-S purification processes.

Parameter	Scale-Up Experiment 1				Scale-Up Experiment 2			
	Harvested sup.	Endonuclease + clarification	TFF I	TFF II	Harvested sup.	Endonuclease + clarification	TFF I	TFF II
Titer per run (10^{10} PFU)	–	9.9 ± 1.9	6.1 ± 1	30	–	38 ± 7	21 ± 3	102
Recovery (%)	–	83	52	42	–	80	44	35
Total titer (10^{10} PFU)	71	59	37	30	289	231	127	102
Total Vero HCP (mg)	524.7	366.4	112.5	18.2	523	414	152	73
PFU/mg Vero HCP	1.3×10^9	1.6×10^9	3.2×10^9	1.6×10^{10}	5.5×10^9	5.5×10^9	8.3×10^9	1.1×10^{10}
Vero HCP purification factor[a]	1×	1.2×	2.4×	12.2×	1×	1×	1.5×	2.1×
Total hc-DNA (μg)	1,484	12	8.5	2	9,800	80.2	24.4	5
PFU/μg hc-DNA	4.8×10^8	5×10^{10}	4.3×10^{10}	1.5×10^{11}	3×10^8	2.9×10^{10}	5.2×10^{10}	2×10^{11}
hc-DNA purification factor[a]	1×	103.7×	90.3×	313.5×	1×	97.7×	176.3×	692×

[a] Purification factors were calculated based on the starting harvested supernatant (sup.).

HCPs were removed during the clarification, 40–50% during the first TFF, and 15–18% during the second TFF. Overall, 86–97% of the HCPs were removed during the three stages. However, taking into consideration the recovery of infectious viral particles, the resulting HCP purification factor was low (approximately 2) except for the second TFF in scale-up experiment 1 (12.2). The results of the residual hc-DNA revealed that 94–96% of the hc-DNA was removed during the endonuclease-digestion and clarification, and the remaining 4–6%, was removed during the first and second TFF. Overall, 99% of the hc-DNA were removed during the 3 stages used during the scale-up experiments.

The residual levels of HCPs after the second TFF stage were 26,000 and 109,000 ng/ml in scale-up experiments 1 and 2, respectively. Although no clear specifications for residual levels of HCPs were established by regulatory agencies, acceptable HCP levels are usually in the range of a few hundreds of ng per dose [33]. Thus, further advanced unit operations, including purification and polishing, are required to meet the acceptable HCP levels. Advanced unit operations of viral vaccines are typically performed by chromatography using three different types of stationary phases: packed beds, membrane adsorbers, and monoliths, implemented in size-exclusion, ion exchange, affinity, hydrophobic-interaction, and mixed-mode chromatography [13]. Chromatography is easily scaled-up with high capacity and offers important advantages such as the use of high flow rates and preservation of labile viruses, importantly advantageous for purification of the rVSV-S [34].

The residual levels of hc-DNA after the second TFF stage were 2.9 ng/ml for scale-up experiment 1 and 5 ng/ml for scale-up experiment 2. The final concentration of the virus in experiment 1 was 3.6×10^8 PFU/ml and 8.3×10^8 PFU/ml in experiment 2. Considering the intended dose of rVSV-S for phase I and II clinical trials which is up to 1×10^8 PFU/dose (https://clinicaltrials.gov/ct2/show/NCT04608305) the residual levels of hc-DNA are substantially lower than the 10 ng per dose recommended by the WHO, the US Food and Drug Administration (FDA), and the European Pharmacopoeia based on case-by-case risk assessment [35].

The results of the scale-up experiments demonstrate that the set of parameters found in the screening experiments are scalable as long as the proportions between the harvested suspension content to membrane surface area ratio, in both clarification filters and HF membranes, are kept.

4. Conclusions

rVSV-S is a vaccine candidate under development by IIBR for controlling the COVID-19 pandemic. The objective of this study was to systematically examine and establish the parameters of the first unit operations of the DSP, namely, endonuclease digestion, clarification, and HF-TFF aimed to remove large particles, reduce the load of impurities, and concentrate and exchange the buffer of viral harvested supernatant. Retaining the infectivity of the rVSV-S during the DSP was challenged by shear sensitivity of the enveloped rVSV-S and its membrane protruding spike protein. Endonuclease digestion and filter train clarification reduced host cell debris, large aggregates, insoluble impurities, and turbidity below 10 NTU and removed 85% of the hc-DNA found in the harvested virus. In a series of screening experiments, we found that a 750 kDa MWCO HF membrane completely rejected the viral particles and that the addition of 4% D-trehalose stabilized rVSV-S during HF-TFF. Considering virus recovery, membrane fouling, and processing time, shear rates in the range of 8,000–12,000 s^{-1} and a low TMP of 0.5–1 were found as the optimal operating conditions for the next step of the DSP scale-up.

Scale-up experiments examined the combined effect of the first unit operations on viral recovery and the removal of critical impurities. A flush of the system after the recovery of the retentate from the first HF-TFF and the second stage of HF-TFF was added to examine its effect on viral recovery and impurity removal. Overall, during the DSP, approximately 40% of viral recovery was obtained while 86–97% of the HCPs were removed and the regulatory requirements of less than 10 ng host cell DNA per dose were met. The addition of the second stage of HF-TFF reduced viral recovery by 10% while removing 15–18% of the total HCPs. The addition of the second TFF stage to a complete downstream manufacturing process should be considered based on its specific contribution relative to the next advanced unit operations (purification and polishing).

The data from the bioprocess developed and reported here showed that by optimizing the shear rate, the TMP, and the sugar additives, the effective recovery of concentrated rVSV-S and simultaneous removal of significant amounts of HCPs and hc-DNA can be achieved. The application of these findings will set the foundation for the development of a complete downstream manufacturing process that includes the subsequent purification and polishing unit operations (i.e. chromatography) [21] for clinical preparations of rVSV-S. Additionally, the results from this study will contribute to the knowledge of the DSP of other vaccines based on the rVSV platform.

Declaration of Competing Interest

The authors declare that they have no known competing financial interests or personal relationships that could have appeared to influence the work reported in this paper.

Acknowledgements

We thank Dr. Chanoch Kronman for the review of this manuscript.

References

[1] Le TT, Cramer JP, Chen R, Mayhew S. Evolution of the COVID-19 vaccine development landscape. Nat Rev Drug Discov 2020;19:667–8. https://doi.org/10.1038/d41573-020-00151-8.
[2] Koirala A, Joo YJ, Khatami A, Chiu C, Britton PN. Vaccines for COVID-19: The current state of play. Paediatr Respir Rev 2020;35:43–9. https://doi.org/10.1016/j.prrv.2020.06.010.
[3] Lichty BD, Power AT, Stojdl DF, Bell JC. Vesicular stomatitis virus: Re-inventing the bullet. Trends Mol Med 2004;10:210–6. https://doi.org/10.1016/j.molmed.2004.03.003.
[4] Ge P, Tsao J, Schein S, Green TJ, Luo M, Zhou ZH. Cryo-EM model of the bullet-shaped vesicular stomatitis virus. Science 2010;327:689–93. https://doi.org/10.1126/science.1181766.
[5] McSharry JJ. The lipid envelope and chemical composition of rhabdoviruses. Rhabdoviruses, vol. 1, CRC Press; 2018, p. 107–17. https://doi.org/10.1201/9781351076388.
[6] Fathi A, Dahlke C, Addo MM. Recombinant vesicular stomatitis virus vector vaccines for WHO blueprint priority pathogens. Hum Vaccines Immunother 2019;15:2269–85. https://doi.org/10.1080/21645515.2019.1649532.
[7] Monath TP, Fast PE, Modjarrad K, Clarke DK, Martin BK, Fusco J, et al. rVSVΔG-ZEBOV-GP (also designated V920) recombinant vesicular stomatitis virus pseudotyped with Ebola Zaire Glycoprotein: Standardized template with key considerations for a risk/benefit assessment. Vaccine X 2019;1:. https://doi.org/10.1016/j.jvacx.2019.100009100009.
[8] Zemp F, Rajwani J, Mahoney DJ. Rhabdoviruses as vaccine platforms for infectious disease and cancer. Biotechnol Genet Eng Rev 2018;34:122–38. https://doi.org/10.1080/02648725.2018.1474320.
[9] Yahalom-Ronen Y, Tamir H, Melamed S, Politi B, Shifman O, Achdout H, et al. A single dose of recombinant VSV-ΔG-spike vaccine provides protection against SARS-CoV-2 challenge. Nat Commun 2020;11. https://doi.org/10.1038/s41467-020-20228-7.
[10] Letko M, Marzi A, Munster V. Functional assessment of cell entry and receptor usage for SARS-CoV-2 and other lineage B betacoronaviruses. Nat Microbiol 2020;5:562–9. https://doi.org/10.1038/s41564-020-0688-y.
[11] Huang Y, Yang C, Xu XF, Xu W, Liu SW. Structural and functional properties of SARS-CoV-2 spike protein: potential antivirus drug development for COVID-19. Acta Pharmacol Sin 2020;41:1141–9. https://doi.org/10.1038/s41401-020-0485-4.
[12] Case JB, Rothlauf PW, Chen RE, Kafai NM, Fox JM, Smith BK, et al. Replication-Competent Vesicular Stomatitis Virus Vaccine Vector Protects against SARS-CoV-2-Mediated Pathogenesis in Mice. Cell Host Microbe 2020;28:465–474. e4. https://doi.org/10.1016/j.chom.2020.07.018.
[13] Wolf MW, Reichl U. Downstream processing of cell culture-derived virus particles. Expert Rev Vaccines 2011;10:1451–75. https://doi.org/10.1586/erv.11.111.
[14] Ausubel LJ, Meseck M, Derecho I, Lopez P, Knoblauch C, McMahon R, et al. Current good manufacturing practice production of an oncolytic recombinant vesicular stomatitis viral vector for cancer treatment. Hum Gene Ther 2011;22:489–97. https://doi.org/10.1089/hum.2010.159.
[15] Kang Y, Cutler MW, Ouattara AA, Syvertsen KE. Purification processes for isolating purified vesicular stomatitis virus from cell culture 2011:WO Pat. WO/2007/123,961, 2007. https://patents.google.com/patent/EP2007883B1/en.
[16] Federspiel MJ, Wegman TR, Langfield KK, Walker HJ, Stephan SA. Rhabdoviridae virus preparations 2010:U.S. Patent Application No. 12/628,789.5-1. https://patentimages.storage.googleapis.com/3b/c9/82/c283c7b24afe69/US20100019677A1.pdf.
[17] Nestola P, Martins DL, Peixoto C, Roederstein S, Schleuss T, Alves PM, et al. Evaluation of novel large cut-off ultrafiltration membranes for adenovirus serotype 5 (Ad5) concentration. PLoS ONE 2014;9:. https://doi.org/10.1371/journal.pone.0115802e115802.
[18] de las Mercedes Segura M, Kamen A, Garnier A. Downstream processing of oncoretroviral and lentiviral gene therapy vectors. Biotechnol Adv 2006;24:321–37. https://doi.org/10.1016/j.biotechadv.2005.12.001.
[19] Nestola P, Peixoto C, Silva RRJS, Alves PM, Mota JPB, Carrondo MJT. Improved virus purification processes for vaccines and gene therapy. Biotechnol Bioeng 2015;112:843–57. https://doi.org/10.1002/bit.25545.
[20] Negrete A, Pai A, Shiloach J. Use of hollow fiber tangential flow filtration for the recovery and concentration of HIV virus-like particles produced in insect cells. J Virol Methods 2014;195:240–6. https://doi.org/10.1016/j.jviromet.2013.10.017.
[21] Lerer Elad, Oren Ziv, Kafri Yaron, Adar Yaakov, Toister Einat, Cherry Lilach, Lupu Edith, Monash Arik, Levy Rona, Dor Eyal, Epstein Eyal, Levin Lilach, Girshengorn Meni, Natan Niva, Ran Zichel AM. Highly Efficient Purification of Recombinant VSV-ΔG-spike Vaccine Against SARS-CoV-2 by Flow-through Chromatography. BioTech J 2021;10:22. https://doi.org/10.3390/biotech10040022.
[22] Gagnon P, Nian R, Lee J, Tan L, Latiff SMA, Lim CL, et al. Nonspecific interactions of chromatin with immunoglobulin G and protein A, and their impact on purification performance. J Chromatogr A 2014;1340:68–78. https://doi.org/10.1016/j.chroma.2014.03.010.
[23] Konz JO, Lee AL, Lewis JA, Sagar SL. Development of a purification process for adenovirus: Controlling virus aggregation to improve the clearance of host cell DNA. Biotechnol Prog 2005;21:466–72. https://doi.org/10.1021/bp049644r.
[24] Vellinga J, Smith JP, Lipiec A, Majhen D, Lemckert A, Van Ooij M, et al. Challenges in manufacturing adenoviral vectors for global vaccine product deployment. Hum Gene Ther 2014;25:318–27. https://doi.org/10.1089/hum.2014.007.
[25] Besnard L, Fabre V, Fettig M, Gousseinov E, Kawakami Y, Laroudie N, et al. Clarification of vaccines: An overview of filter based technology trends and best practices. Biotechnol Adv 2016;34:1–13. https://doi.org/10.1016/j.biotechadv.2015.11.005.
[26] Raghavan B, Collins M, Walls S, Lambropoulos A, Bergheim-Pietza S. Optimizing the clarification of industrial scale viral vector culture for gene therapy. Cell Gene Ther Insights 2019;5:1311–22. https://doi.org/10.18609/cgti.2019.137.
[27] Lothert K, Pagallies F, Eilts F, Sivanesapillai A, Hardt M, Moebus A, et al. A scalable downstream process for the purification of the cell culture-derived Orf virus for human or veterinary applications. J Biotechnol 2020;323:221–30. https://doi.org/10.1016/j.jbiotec.2020.08.014.
[28] Carvalho SB, Silva RJS, Moreira AS, Cunha B, Clemente JJ, Alves PM, et al. Efficient filtration strategies for the clarification of influenza virus-like particles derived from insect cells. Sep Purif Technol 2019;218:81–8. https://doi.org/10.1016/j.seppur.2019.02.040.
[29] Kalyan NK, Yurgelonis I, Hendry RM, Cutler MW, Syvertsen KE. Genetically Modified Attenuated Vesicular Stomatitis Virus, Compositions and Methods of use Thereof. WO2009082664A3 US 2009/0175906 A1, 2009. https://doi.org/https://patents.google.com/patent/US20090175906/en.
[30] KANG Y. Purification Processes for Isolating Purified Vesicular Stomatitis Virus From Cell Culture. WO Pat. WO/2007/123,961, 2007. https://doi.org/https://patents.google.com/patent/EP2007883B1/en.
[31] Ohtake S, Wang YJ. Trehalose: Current use and future applications. J Pharm Sci 2011;100:2020–53. https://doi.org/10.1002/jps.22458.
[32] Michalsky R, Passarelli AL, Pfromm PH, Czermak P. Concentration of the baculovirus Autographa californica M nucleopolyhedrovirus (AcMNPV) by ultrafiltration. Desalination 2010;250:1125–7. https://doi.org/10.1016/j.desal.2009.09.123.
[33] Pato TP, Souza MCO, Mattos DA, Caride E, Ferreira DF, Gaspar LP, et al. Purification of yellow fever virus produced in Vero cells for inactivated vaccine manufacture. Vaccine 2019;37:3214–20. https://doi.org/10.1016/j.vaccine.2019.04.077.
[34] Morenweiser R. Downstream processing of viral vectors and vaccines. Gene Ther 2005;12:S103–10. https://doi.org/10.1038/sj.gt.3302624.
[35] Vernay O, Sarcey E, Detrez V, Abachin E, Riou P, Mouterde B, et al. Comparative analysis of the performance of residual host cell DNA assays for viral vaccines produced in Vero cells. J Virol Methods 2019;268:9–16. https://doi.org/10.1016/j.jviromet.2019.01.001.